REMOTE DETECTION OF WATER AND NUTRITIONAL STATUS OF SOYBEANS USING UAV-BASED IMAGES

Aderson S. de Andrade Junior[1]*, Silvestre P. da Silva[2], Ingrid S. Setúbal[2], Henrique A. de Souza[1], Paulo F. de M. J. Vieira[1]

[1]*Corresponding author. Embrapa Meio-Norte/ Teresina - PI, Brazil.
E-mail: aderson.andrade@embrapa.br | ORCID ID: https://orcid.org/0000-0002-0619-1851

KEYWORDS

Glycine max L., RPA, vegetation indexes, gas exchange.

ABSTRACT

Digital aerial images obtained by cameras embedded in remotely piloted aircraft (RPA) have been used to detect and monitor abiotic stresses in soybeans, such as water and nutritional deficiencies. This study aimed to evaluate the ability of vegetation indexes (VIs) from RPA images to remotely detect water and nutritional status in two soybean cultivars for nitrogen. The soybean cultivars BONUS and BRS-8980 were evaluated at the phenological stages R5 and R3 (beginning of seed enlargement), respectively. To do so, plants were subjected to two water regimes (100% ETc and 50% ETc) and two nitrogen (N) supplementation levels (with and without). Thirty-five VIs from multispectral aerial images were evaluated and correlated with stomatal conductance (gs) and leaf N content (NF) measurements. Near-infrared (NIR) spectral band, enhanced vegetation index (EVI), soil-adjusted vegetation index (SAVI), and renormalized difference vegetation index (RDVI) showed linear correlation (p<0.001) with gs, standing out as promising indexes for detection of soybean water status. In turn, simplified canopy chlorophyll content index (SCCCI), red-edge chlorophyll index (RECI), green ratio vegetation index (GRVI), and chlorophyll vegetation index (CVI) were correlated with NF (p<0.001), thus being considered promising for the detection of leaf N content in soybeans.

INTRODUCTION

According to precision agriculture principles, high-precision and low-cost estimates of plant biophysical and biochemical parameters are important to improve management practices and productive potential in farming systems (Vibhute & Bodhe, 2012). High throughput and spatial accuracy of these estimates using aerial images from remotely piloted aircraft (RPA) can assist in evaluating genotype behavior, management practices, and impacts of biotic and abiotic stresses, thus contributing to decision-making by farmers (Franchini et al., 2018).

Digital aerial images from RPAs have been used to detect and monitor spatial and temporal variability in croplands (Barbedo, 2019). Studies have demonstrated the viability of aerial images at some crop development stages to spatialize information about vegetative vigor, nutritional status, the incidence of pests and diseases, weed infestation, and productive potential (Tetila et al., 2017; Franchini et al., 2018; Barbedo, 2019).

Drought stress has reduced global soybean yields by more than 50% annually (Wang et al., 2003). The effect of droughts on soybean yields depends on the severity, duration, and timing of stress regarding the crop growth stage (Brar et al., 1990). Soybean is most susceptible to drought stress during its reproductive stage (Wijewardana et al., 2018, 2019b); however, when under long-term severe water stress during vegetative growth, substantial yield losses can be caused (Machado et al., 2020).

Drought effects on soybean physiological and biochemical changes are not clearly understood yet (Manalavan et al., 2009). Soil moisture stress may induce several morpho-physiological and biochemical responses that subsequently inhibit growth, lower photosynthesis,

reduce stomatal conductance and transpiration, decrease chlorophyll contents, and cause changes in proteomics (Reddy et al., 2004; Wijewardana et al., 2019a).

Leaf nitrogen (N) contents are directly correlated with chlorophyll production, thus affecting crop growth and yield. Farmers have used soil plant analysis development (SPAD) devices to estimate chlorophyll contents in plants. However, large-scale crop monitoring through SPAD is time-consuming and demanding; therefore, unmanned aerial vehicles (UAV) are recommended for estimating leaf N contents in crops using multispectral imagery (Colorado et al., 2020).

Some studies have been conducted on the use of aerial images to detect and monitor abiotic stresses, especially water and nutritional stresses in soybeans (Hoyos-Villegas & Fritschi, 2013; Yu et al., 2016; Maimaitijiang et al., 2017; Franchini et al., 2018; Wijewardana et al., 2019b). Regarding nutritional status, Franchini et al. (2018) studied soybean spectral responses to potassium (K) application and observed a correlation between K levels in the soil and modified photochemical reflectance index (mPRI).

Remote detection of water deficit in crops can be performed by the joint use of vegetation indexes, such as NDVI, and leaf canopy temperature measurements from thermal cameras embedded in RPAs (Carvalho et al., 2015; Hoffmann et al., 2016; Crusiol et al., 2017; Sagan et al., 2019; Crusiol et al., 2020). Crusiol et al. (2020) evaluated the use of remote (hyperspectral) and airborne (RGB/NIR and thermal cameras embedded in drones) sensors to detect water deficit in soybeans. They concluded that remote sensors could differentiate water conditions in soybean cultivars, improving management and decision-making in terms of crop practices.

Some vegetation indexes (VIs) from multispectral images are related to crop water status (Gago et al., 2015). Baluja et al. (2012) found a significant correlation between VIs from multispectral imagery (e.g., NDVI and OSAVI) and vine water stress indexes (e.g., stomatal conductance). Likewise, Wijewardana et al. (2019b) evaluated the use of vegetation indexes to detect water status in soybeans and concluded that NDVI has a high positive linear correlation with leaf water potential and stomatal conductance. However, the use of multispectral indexes with physiological and thermal indicators of plant water status still needs validation to replace aerial thermography, which is more expensive (Bian et al., 2019).

Given the above, we hypothesize that soybean water and nutritional status can be detected using vegetation indexes from aerial images derived from multispectral cameras embedded in RPAs. Thus, this study aimed to evaluate the ability of vegetation indexes from aerial images of a multispectral camera embedded in a remotely piloted aircraft (RPA) to remotely detect the water and nutritional status of two soybean cultivars regarding N contents.

MATERIAL AND METHODS

The experiment was conducted in the experimental area of Embrapa Meio-Norte in Teresina, PI, Brazil (05°05' S, 42°49' W, and 74.4-m altitude), from July to November 2019 (Figure 1). The historical annual averages of temperature and cumulative rainfall are 27.4 °C and 1,325 mm, respectively, with rains concentrated between January and May (INMET, 2019). During the experiment, mean maximum and minimum temperatures and cumulative rainfall were 29.44 °C, 27.6 °C, and 0.11 mm, respectively (INMET, 2019). The local climate is defined as *Aw* according to the Köppen classification, with a rainy season in the summer and a dry season in the winter (Medeiros et al., 2020). The soil in the experimental area is classified as eutrophic Red Yellow Argisol (Melo et al., 2014) (Table 1).

The experiment was carried out using two soybean cultivars: 1) BONUS, with indeterminate growth habit, maturity group (MG) 7.9, a cycle of 105-122 days; and 2) BRS-8980, with determinate growth habit, MG 8.9, and a cycle of 125-136 days. The design adopted was a randomized block arranged in a split-plot scheme, in which plots comprised two water regimes (WR): deficit irrigation (50% crop evapotranspiration [ETc] replacement) and full irrigation (100% ETc replacement), while subplots consisted of two nitrogen (N) supplementation levels (NS): without N (N0) and with N (N1; 1,000 kg ha^{-1}). Therefore, four treatments (I0N0, I0N1, I1N0, and I1N1) were performed, with five replicates each.

Sowing was performed manually on July 23, 2019, by distributing 20 seeds per meter along furrows. Before sowing, seeds were inoculated with *Bradyrhizobium japonicum* (SEMIA 5079 and 5080) at a ratio of 100 mL inoculant to 7 kg seeds. After germination, seedlings were thinned out, leaving 10 to 12 plants per meter. For the cultivar BONUS, each plot contained twenty 6-m rows spaced 0.5 m apart (60 m²) and a 24-m² useful area. For the cultivar BRS-8980, each plot contained twenty 4.5-m rows spaced 0.5 m apart (45 m²) and an 18-m² useful area.
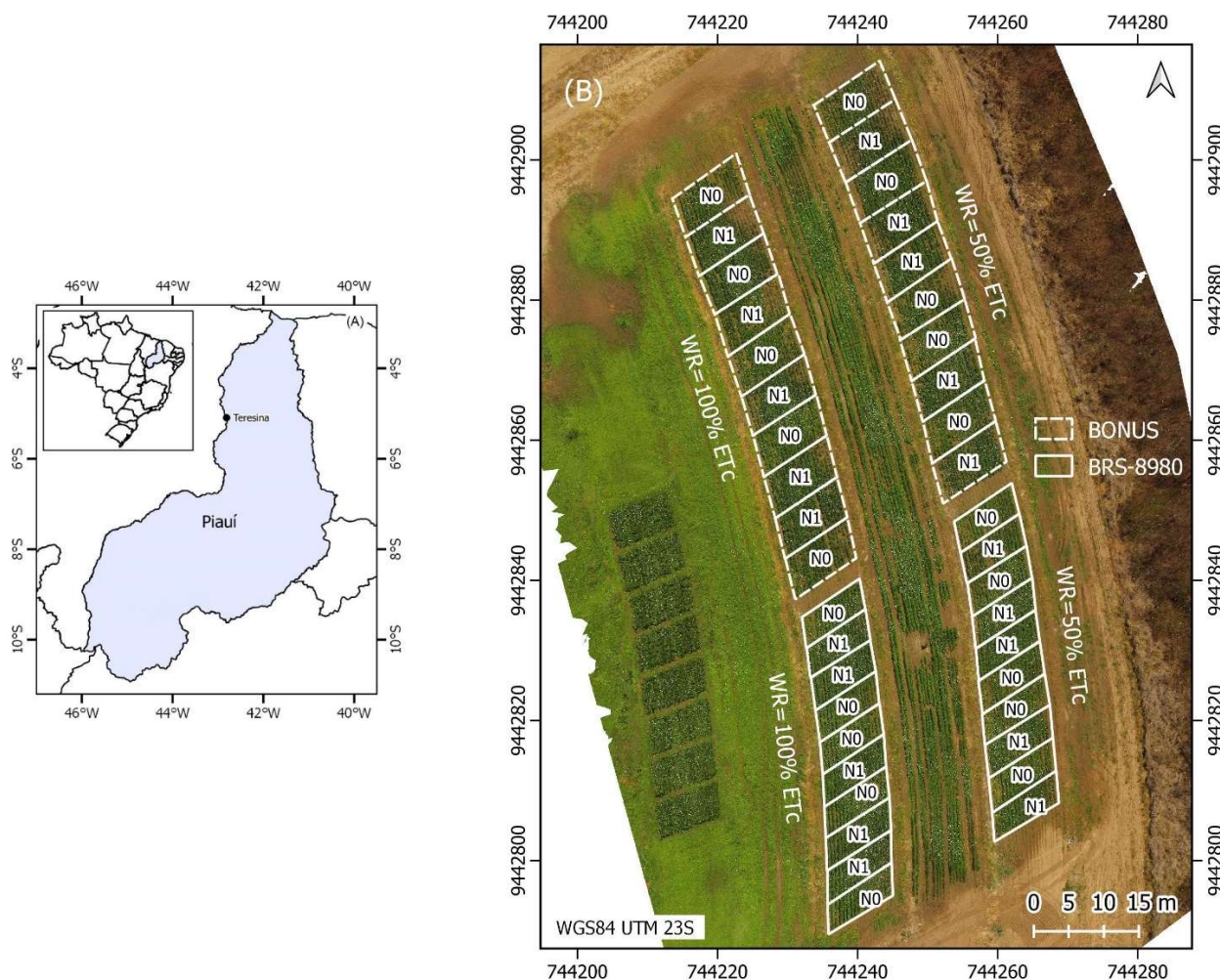
FIGURE 1. Location (A) and detailing (B) of the experimental area. Teresina, PI, 2019.

TABLE 1. Chemical properties and soil granulometry of the experimental area. Teresina, PI, 2019.

Depth Layer (m)	Sand	Fine Sand	Silt	Clay	Textural Classification
	------------------------- g kg⁻¹ -------------------------				
0.0-0.2	267.3	470.6	116.0	146.1	Loam-sandy
0.2-0.4	231.6	424.0	105.5	238.9	Loam-clay-sandy

Depth Layer (m)	P	K	Ca	Mg	H+Al	SB	CEC	OM	S	pH (CaCl$_2$)
	mg/dm³	---------------------- cmolc/dm³ --------------------						dag/kg	%	
0.0-0.2	10.15	0.23	2.40	0.83	1.18	3.45	4.63	1.03	74.5	5.50
0.2-0.4	5.41	0.22	2.63	0.83	1.34	3.68	5.01	0.91	73.4	5.38

P: phosphorus; K: potassium; Ca: calcium; Mg: magnesium; H+Al: potential acidity; SB: sum of bases; CEC: cation exchange capacity; OM: organic matter; V%: base saturation; pH (CaCl$_2$): pH in calcium chloride.

Fertilization was managed based on the soil chemical analysis. Nitrogen (urea), phosphorus (simple superphosphate), and potassium (potassium chloride) were applied to the soil, while micronutrients were sprayed on leaves (Silva, 2021). The dose of 1,000 kg N ha^{-1} was selected to meet soybean N demands throughout the crop season so that both cultivars could express their maximum yield potentials (6 Mg ha^{-1} expected yield). To that end, for each Mg soybean produced, 80 kg N ha^{-1} were estimated, at an N fertilization efficiency of 50% (Hungria et al., 2001).

Irrigation was managed to replace crop evapotranspiration (ETc), using the Penman-Monteith estimated reference evapotranspiration (ETo) and soybean FAO crop coefficients – Kc (Allen et al., 1998). Climatic data (global solar radiation [MJ m^{-2}], air temperature [°C], relative air humidity [%], and wind speed [ms^{-1}]) were acquired from an automatic agro-meteorological station, which is 500 m away from the experimental area. Irrigation was performed using a fixed conventional sprinkler system, with 24 sprinklers spaced at 12 m x 12 m. Irrigation depth was controlled by installing two blocks of 12 collectors each, one for each water regime (WR), spaced 3 m between lateral sprinkler lines and in the center of the experimental area. Soil moisture was monitored using Campbell's CS616

soil moisture probes, with three rods for each WR, two for the 0.0-0.3 m and one for the 0.3-0.6 m depth layers, with continuous measures recorded in a CR1000 datalogger.

WRs were applied as a function of soybean development stages (Thomas, 2018 adapted from Fehr & Caviness, 1977). From sowing to stage V3 (three main stem nodes with fully developed leaves), irrigation was fully applied in both treatments (100% ETc). Thereafter, from V4 (four main stem nodes with fully developed leaves) to R5 (beginning of seed enlargement), both WRs were performed, namely replacing 50 and 100% ETc. After R5, irrigation was again fully applied in both treatments (100% ETc).

The imagery was acquired from a hexacopter unmanned aerial vehicle (UAV), model X800, produced by XFly Brasil (XFly Tecnologia, Bauru, Brazil). A flight was performed on September 24, 2019, 62 days after soybean sowing - DAS (at R5 stage for BONUS and R3 for BRS-8980), between 11:00 am and 12:00 pm. The flight was planned using the software Pix4D Capture® (www.pix4d.com) to ensure image capture with 80% side and front overlap. The flight line was maintained at 30 meters above ground level, with a GSD (ground sample distance) of ≈ 1.5 cm.

Multispectral images were acquired by a Micasense sensor, model RedEdge®, capable of capturing five spectral bands simultaneously: blue (475 nm), green (560 nm), red (668 nm), Red Edge (717 nm), and NIR (840 nm). The generated images were georeferenced and corrected using GPS and a solar radiation sensor installed on the top of the aircraft, respectively. A radiometric calibration standard was also used to correct the images, which were saved in 16-bit tiff format. Then, orthomosaic images were created, using the Pix4D Mapper® software.

The orthomosaic generated underwent a supervised classification process (maximum likelihood method), allowing the rasterization of the orthomosaic into two classes (soil and leaves). This enabled the removal of pixels classified as mosaic soil, ensuring that the VIs had been estimated only with pixels classified as leaves. The process was performed using the Semi-Automatic Classification (SCP) plug-in of QGIS v. 218 (QGIS, 2016).

The spectral responses of soybeans to the treatments were quantified using 35 VIs from multispectral image bands (R, G, B, Red Edge, and NIR) (Table 2). The multispectral indexes were estimated using the QGIS raster calculator (QGIS, 2016). The VI values of each subplot were extracted with the QGIS zonal statistics plugin (QGIS, 2016). To this end, the vector layer of the subplots was used, containing only the areas classified as leaves.

TABLE 2. Spectral bands and vegetation indexes evaluated in the study.

Band/Index	Acronym	Equation	Reference
Green band	GREEN	/	/
Red band	RED	/	/
Red-Edge band	RED-EDGE	/	/
NIR band	NIR	/	/
Chlorophyll index red	CI-RED	$\dfrac{R_n}{R_r} - 1$	Gitelson et al. (2005)
Chlorophyll vegetation index	CVI	$\dfrac{R_n R_r}{R_g{}^2}$	Vincini et al. (2008)
Enhanced vegetation index	EVI	$\dfrac{2.5(R_n - R_r)}{R_n + 6R_r - 7.5R_b + 1}$	Huete et al. (2002)
Two-band enhanced vegetation index	EVI2	$\dfrac{2.5(R_n - R_r)}{R_n + 2.4R_r + 1}$	Jiang et al. (2008)
Excess green red	EXGR	$\dfrac{3R_g - 2.4R_r - R_b}{R_r + R_g + R_b}$	Meyer & Camargo Neto (2008)
Green chlorophyll index	GCI	$\dfrac{R_n}{R_g} - 1$	Gitelson et al. (2005)
Green leaf index	GLI	$\dfrac{2R_g - R_r - R_b}{2R_g + R_r + R_b}$	Hunt et al. (2013)
Green normalized difference vegetation	GNDVI	$\dfrac{R_n - R_g}{R_n + R_g}$	Hunt e Daughtry (2018)
Green ratio vegetation index	GRVI	$\dfrac{R_n}{R_g}$	Sripada et al. (2006)
Modified excess green	MEXG	$1.262R_g - 0.884R_r - 0.311R_b$	Burgos-Artizzu et al. (2011)
Modified normalized green red difference	MNGRD	$\dfrac{R_g^2 - R_r^2}{R_g^2 + R_r^2}$	Bendig et al. (2015)
Normalized difference Red-Edge	NDRE	$\dfrac{R_n - R_{RE}}{R_n + R_{RE}}$	Wang et al. (2019)

Normalized difference Red-Edge index	NDREI	$\dfrac{R_{RE} - R_g}{R_{RE} + R_g}$	Hassan et al. (2018)
Normalized difference vegetation index	NDVI	$\dfrac{R_n - R_r}{R_n + R_r}$	Gitelson et al. (2005)
Normalized green	NG	$\dfrac{R_g}{R_r + R_g + R_b}$	Woebbecke et al. (1995)
Normalized green red difference	NGRD	$\dfrac{R_g - R_r}{R_g + R_r}$	Hamuda et al. (2016)
Optimized Soil Adjusted Vegetation Index	OSAVI	$\dfrac{R_n - R_r}{R_n + R_r + 0.16}$	Rondeaux et al. (1996)
Pigment-specific normalized difference index	PSND	$\dfrac{R_n - R_b}{R_n + R_b}$	Blackburn (1998)
Renormalized Difference Vegetation Index	RDVI	$\dfrac{R_n - R_r}{(R_n - R_r)^{0.5}}$	Roujean & Breon (1995)
Red-Edge chlorophyll index	RECI	$\dfrac{R_n}{R_{RE}} - 1$	Gitelson et al. (2005)
Red-green difference	GDPR	$R_r - R_g$	Sanjerehei (2014)
Ratio vegetation index	RVI	$\dfrac{R_n}{R_r}$	Tucker (1979)
Soil Adjusted Vegetation Index	SAVI	$\dfrac{1.5(R_n - R_r)}{(R_n + R_r + 0.5)}$	Zhong et al. (2019)
Simplified canopy chlorophyll content index	SCCCI	$\dfrac{NDRE}{NDVI}$	Raper & Varco (2015)
Transformed chlorophyll absorption in Nir index	TCARI	$3\left[(R_n - R_r) - 0.2(R_n - R_g)\left(\dfrac{R_n}{R_r}\right)\right]$	Haboudane et al. (2002)
TCARI/OSAVI index	TCARI-OSAVI	$\dfrac{TCARI}{OSAVI}$	Haboudane et al. (2002)
Transformed chlorophyll absorption in the Red-edge index	TCARI-RE	$3\left[(R_{RE} - R_r) - 0.2(R_{RE} - R_g)\left(\dfrac{R_{RE}}{R_r}\right)\right]$	Daughtry et al. (2000)
TCARI/OSAVI-RE index	TCARI-OSAVI-RE	$\dfrac{TCARI_{RE}}{OSAVI}$	Daughtry et al. (2000)
Triangular greenness index	GIT	$R_g - (0.39R_r) - (0.61R_b)$	Hunt et al. (2011)
Wide dynamic range vegetation index	WDRVI	$\dfrac{(0.12R_n) - R_r}{(0.12R_n) + R_r}$	Gitelson (2004)
Weighted difference vegetation index	WDVI	$R_n - R_r\left(\dfrac{R'_n}{R'_r}\right)$	Clevers (1989)

R_n: Spectral reflectance - near infrared (840 nm); R_g: Spectral reflectance - green (560 nm); R_{RE}: Spectral reflectance - near red (717 nm); R_r: Spectral reflectance red (668 nm) and R_b: Spectral reflectance - blue (475 nm); R'_n: Spectral reflectance - near infrared (soil); R'_r: Red spectral reflectance (soil).

Gas exchange measurements were performed in the electromagnetic spectrum IR region, using a portable gas analyzer LI-COR model 6400XT (LI-COR, Lincoln, NE, USA), equipped with a measuring chamber and artificial lighting LI-COR model 6400-02B. The measurements were performed on the same day of the flight, using one plant per subplot of the cultivar BRS-8980 at the R3 stage, between 8:00 and 10:00 am, under cloudless conditions. The extracted data provided by Open Software version 6.3 were as follows: A: Net CO_2 assimilation rate (micromol CO_2 m^{-2} s^{-1}), gs: stomatal conductance (mmol H_2O m^{-2} s^{-1}), and E: transpiration rate (mmol H_2O m^{-2} s^{-1}).

Leaf N accumulation (NF) was quantified on the same day of the flight in plants of the cultivar BONUS at the R5 stage. Four plants were collected from each subplot and split into organs (stem, leaves, reproductive structures, and grains), washed in running and distilled water, and then dried in a forced-air oven at 65 °C until reaching constant weight for subsequent dry biomass quantification. After

drying, the samples were processed and used for plant tissue chemical analysis for N by the Kjeldahl method (Teixeira et al., 2017). Leaf dry biomass and N content data were used to estimate leaf N accumulations per unit area (g m^{-2}), with the dry biomass per area being estimated based on each subplot stand.

The data were subjected to the Shapiro-Wilk test (normality of errors) and Cochran's t-test (homogeneity of variance). Once the basic normality criteria were met, the data were subjected to analysis of variance, mean comparison test (Tukey's test) at 5% probability, Pearson's correlation (r), and regression between vegetation indexes and measurements of stomatal conductance (gs) and leaf N accumulation (NF). The statistical analyses were performed using the ExpDes.pt package of the R software (Ferreira et al., 2018). The degree of fit of the linear regression models for estimating gs and NF was evaluated by the coefficient of determination (R^2) (equation 1) and standard error of the regression (SEE), which represent the average distance of the observed values

concerning the line of the regression (equation 2). For this purpose, the Excel Real Statistics Resource Pack (version 7.6) supplement (Zaiontz, 2020) was used.

$$R^2 = \frac{\sum_{i=1}^{n}(\hat{Y}_i - \hat{Y}_m)^2}{\sum_{i=1}^{n}(Y_i - \overline{Y_i})^2} \qquad (1)$$

$$SEE = \sqrt{\frac{\sum_{i=1}^{n}(Y_i - \hat{Y}_i)^2}{n-2}} \qquad (2)$$

Where:

   n - number of observations;

   Y_i - gs and NF values measured in the field;

   $\hat{Y}_i$ - gs and NF values estimated by the regression models,

$\hat{Y}_m$ - means of gs and NF estimated by the regression models.

RESULTS AND DISCUSSION

Irrigation depths and soil moisture

Table 3 shows the accumulated irrigation depths (mm) for each water regime (WR) applied during the soybean season. From the beginning of irrigation until the application of differentiated WRs (IT), accumulated irrigation depths were 125.3 and 127.1 mm for treatments with 50 and 100% ETc, respectively. Therefore, during the initial period, both treatments received similar irrigation depths regardless of the soybean cultivar.

TABLE 3. Accumulated irrigation depths (mm) for each water regime applied during the soybean crop season. Teresina, PI, 2019.

WR (% ETc)	S – IT	IT – TT	TT – TI	Season
BONUS				
50 % ETc	125.3	132.9	87.6	345.8
100 % ETc	127.1	252.8	85.3	465,2
BRS-8980				
50 % ETc	125.3	174.6	56.1	356.0
100 % ETc	127.1	326.5	57.7	511.3

WR: water regime (% ETc); S: sowing date; IT: beginning of the application of differentiated WRs (40 DAS) (V3); TT: end of the application of differentiated WRs (72 DAS) (R7); TI: end of irrigation application (93 – DAS for BONUS, and 103 DAS for BRS-8980) (R8).

During the application of differentiated WRs (IT-TT), treatments with 50% ETc received 132.9 and 174.6 mm, while those with 100% ETc had 252.8 and 326.5 mm for the cultivars BONUS and BRS-8980, respectively. During the IT-TT period, deficit irrigation (50% ETc) corresponded to 47% of the full irrigation (100% ETc) for both soybean cultivars. Thus, irrigation depths were different between the WR evaluated. After the application of differentiated WRs until the end of irrigation (TT-TI), treatments with 50% ETc received 87.6 and 56.1 mm, while those with 100% ETc had 85.3 and 57.7 mm for the cultivars BONUS and BRS-8980, respectively (Table 3). Throughout the crop season, for both soybean cultivars, treatments with 50% ETc received irrigation depths of 345.8 mm for the cultivar BONUS, and 356 mm for the cultivar BRS-8980. Under full irrigation (100% ETc), 465.2 mm were applied for the cultivar BONUS, and 511.3 mm for the cultivar BRS-8980 (Table 3). These irrigation depth differences may be related to each cultivar maturation group, i.e., BONUS (7.9) and BRS-8989 (8.9). In this sense, some studies have pointed out that, depending on soil conditions, climate, sowing date, and cultivars, soybeans may require total irrigation depths from 450 to 850 mm during the crop season to achieve maximum grain yields (Allen et al., 1998).

From the beginning of irrigation until the application of differentiated WRs (IT), the average soil moisture contents in the 0.0-0.3 m depth layer were 13.0 and 14.2% for treatments with 50% and 100% ETc, respectively. In the 0.3-0.6 m depth layer, the soil moisture contents averaged 8.6% for 50% ETc and 10.3% for 100% ETc (Figure 2). These results demonstrate that, before the application of differentiated WRs, the average soil moisture in the 0.0-0.3 m depth layer for both WRs was close to and above the critical level for soybeans (12.5%), thus favoring the full development of the crop.

Throughout the application of differentiated WRs (IT-TT), the average soil moisture in the 0.0-0.3 m depth layer was 9.9 and 14.7% for treatments with 50 and 100% ETc, respectively; in the 0.3-0.6 m depth layer, these contents were 7.7% for 50% ETc and 12.7% for 100% ETc. From the beginning of irrigation until the flight date (62 DAS; at R5 stage for BONUS and R3 for BRS-8980), the average soil moisture contents in the 0.0-0.3 m depth layer were 10.0% and 13.2% for treatments with 50% and 100% ETc, respectively, while in the 0.3-0.6 m depth layer these contents were 7.6% for 50% ETc and 12.3% for 100% ETc (Figure 2).
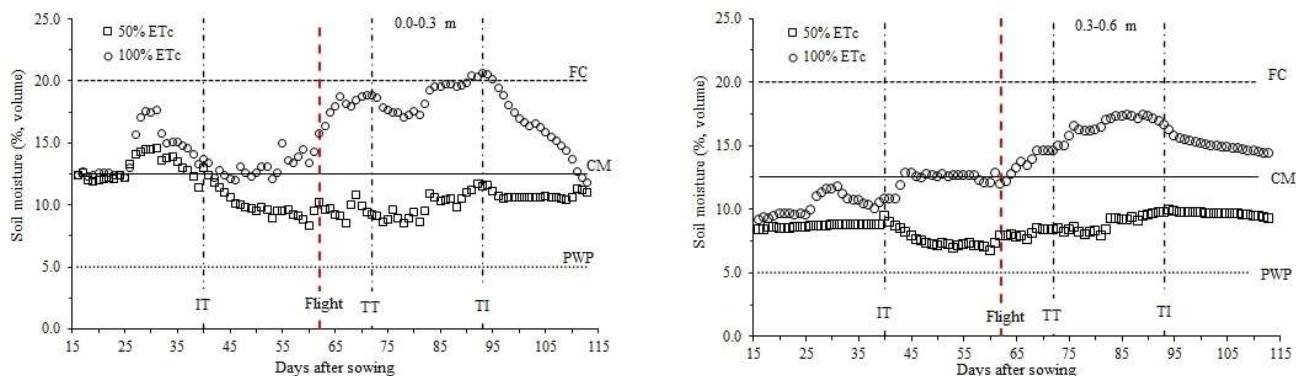
FC: field capacity; CM: critical moisture; PWP: permanent wilting point; TI: beginning of the application of differentiated WR (40 DAS) (V3); TT: end of the application of differentiated WR (72 DAS) (R7); IT: end of irrigation application (93 DAS) (R8); Flight: flight date (62 DAS; at R5 stage for BONUS and R3 for BRS-8980).

FIGURE 2. Soil moisture changes during the soybean crop season in the 0.0-0.3 and 0.3-0.6 m depth layers in response to the applied water regimes (WR). Teresina, PI, 2019.

Our results show that, in both depth layers (0.0-0.3 and 0.3-0.6 m), full irrigation kept soil moisture above critical levels, allowing proper soybean development and production. Conversely, deficit irrigation promoted soil moisture levels below the critical and above the permanent wilting point during the evaluated period, limiting soybean development and grain yields.

Vegetation indexes and gas exchange

Among the gas-exchange-related parameters, for the cultivar BRS-8980, only stomatal conductance (gs) had significant changes ($p<0.01$) in response to the WRs applied. However, no significant effect was observed due to N supplementation levels (NS) or WR*NS interaction (Table 4). Moreover, neither internal CO_2 concentrations nor transpiration showed responses to those parameters.

TABLE 4. F-test for stomatal conductance (gs), leaf nitrogen content (NF), and vegetation indexes (VIs) in response to water regimes (WR) and nitrogen supplementation levels (NS) for the soybean cultivars BRS-8980 and BONUS. Teresina, PI, 2019.

VI	BRS-8980			BONUS			VI	BRS-8980			BONUS		
	WR	NS	WR*NS	WR	NS	WR*NS		WR	NS	WR*NS	WR	NS	WR*NS
gs	**	ns	ns				OSAVI	***	ns	ns	**	ns	ns
NF				*	*	ns	PSND	**	ns	ns	**	*	ns
CI-RED	***	ns	ns	***	ns	ns	RDVI	***	ns	ns	***	ns	ns
CVI	***	***	ns	***	ns	ns	RECI	***	ns	ns	***	ns	ns
EVI	***	ns	ns	***	ns	ns	RED	ns	ns	ns	**	*	ns
EVI2	***	ns	ns	***	ns	ns	RED-EDGE	*	ns	ns	**	*	ns
EXGR	*	***	ns	*	**	ns	GDPR	*	ns	ns	ns	ns	ns
CI	***	**	ns	***	ns	ns	RVI	***	ns	ns	***	ns	ns
GLI	**	***	ns	ns	**	ns	SAVI	***	ns	ns	***	ns	ns
GNDVI	***	*	*	**	ns	ns	SCCCI	***	ns	ns	***	ns	ns
GREEN	*	**	ns	**	ns	*	ICART	***	ns	ns	***	ns	ns
GRVI	***	**	ns	***	ns	ns	TCARI-OSAVI	***	ns	ns	***	ns	ns
MEXG	**	***	ns	**	ns	ns	TCARI-OSAVI-RE	ns	*	ns	**	*	*
MNGRD	ns	***	ns	**	**	ns	TCARI-RE	ns	*	ns	**	*	*
NDRE	***	*	ns	***	ns	ns	GIT	**	***	ns	**	ns	ns
NRDEI	**	*	ns	**	ns	ns	WDRVI	***	ns	ns	**	ns	*
NDVI	***	ns	ns	**	ns	ns	WDRVI-1	***	ns	ns	***	ns	*
NG	**	***	ns	ns	**	ns	WDRVI-2	***	ns	ns	**	ns	ns
NGRD	ns	***	ns	**	**	ns	WDVI	ns	ns	ns	ns	ns	*
NIR	***	ns	ns	***	ns	ns							

WR: ETc-based water regime (50-ETc and 100-ETc); NS: nitrogen supplementation levels (N0 and N1). Significance levels by the F-test: ***: $p <0.001$; **: $p <0.01$; *: $p <0.05$; ns: non-significant.

For the cultivar BRS-8980, except for NGRD, TCARI-OSAVI-RE, TCARI-RE, and WDVI IVs, all the other VIs responded to the applied WRs. On the other hand, for the cultivar BONUS, only GLI, NG, RGD, and WDVI did not respond to this factor. The VIs with a significant F-test had the potential to detect soybean water status; however, the promising VIs were those showing the highest correlations with stomatal conductance measurements performed in the field.

Stomatal conductance (gs) in treatments under full irrigation (690.8 mmol H_2O m^{-2} s^{-1}) was higher than that of treatments under deficient irrigation (487.6 mmol H_2O m^{-2} s^{-1}) (Figure 3). Machado Junior et al. (2017) and Silva et al. (2020) also observed gs reductions in soybeans under soil water restriction. Stomatal conductance was the highest when solar radiation was high and leaf water potential had not yet reached minimum values to induce stomatal closure. Under soil water restriction, soybeans tend to reduce stomatal conductance, as a strategy to avoid water losses to the atmosphere, but reducing photosynthetic activity and hence grain yields (Gorthi et al., 2019).
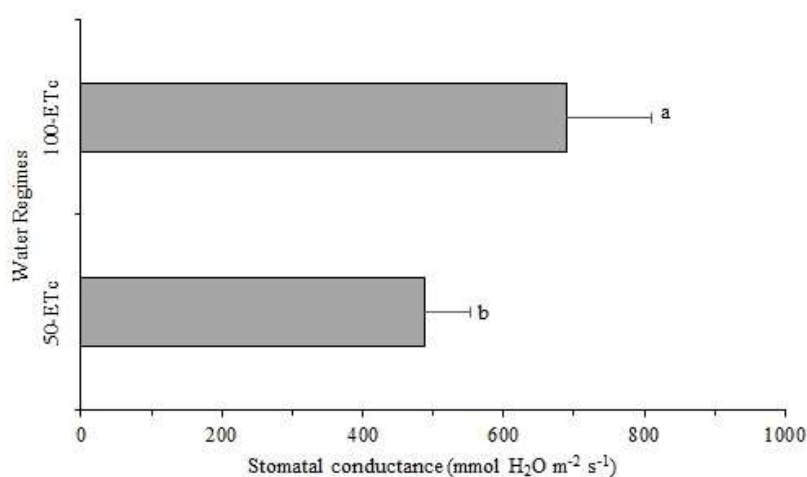
FIGURE 3. Stomatal conductance (cultivar BRS-8980) in response to the water regimes (WR) applied to soybeans. Teresina, PI, 2019.

Chavarria et al. (2015) observed that soil water potentials equal to or below -0.026 MPa cause significant reductions in the photosynthetic activity of soybeans, of the cultivar 'BMX Apolo RR', due to lower gs under water deficiency in the soil. The authors obtained gs equal to 741.0 mmol H_2O m^{-2} s^{-1} under adequate water availability conditions in the soil (-0.004 MPa), while under soil water restriction (-0.026 MPa) it decreased to 426.5 mmol H_2O m^{-2} s^{-1}, which is very close to our values. Karaca et al. (2018) obtained mean values of gs for two soybean cultivars equal to 574.5 mmol H_2O m^{-2} s^{-1} under full irrigation and 251.5 mmol H_2O m^{-2} s^{-1} under water deficit conditions in the soil.

Given the importance of biological N fixation for soybeans, one should note that this process can be compromised by water restriction (Chavarria et al., 2015). Under conditions of water stress, there is a reduction in biological nitrogen fixation and a consequent decrease in photosynthetic rates. Furthermore, due to higher leaf activity and continuous N supply, N_2 fixation slows leaf senescence and increases grain filling in soybean plants (Kaschuk et al., 2010).

The parameter gs showed a significant correlation with several VIs. As the VIs with r≥0.6 are considered promising (Yue et al., 2020), the six best VIs to detect water status were: NIR (r = 0.6779; p<0.001), EVI (r = 0.6741; p <0.01), SAVI (r = 0.6723; p <0.01), RDVI (r = 0.6713; p <0.01), OSAVI (r = 0.6611; p <0.01), and NDRE (r = 0.6294; p <0.01) (Figure 4). A few studies have indicated that VIs using spectral bands in the NIR are the most suitable to detect water status in crops grown in soils under water stress conditions (Elsayed et al., 2015). In our study, EVI, SAVI, RDVI, OSAVI, and NDRE fit the condition established by Elsayed et al. (2015).
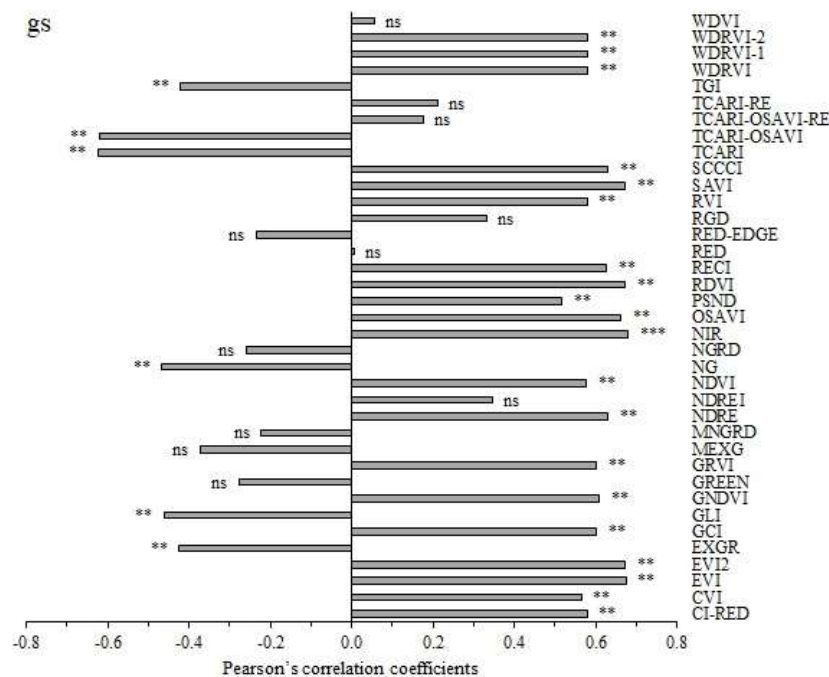
Significance levels by the t-test: ***: p<0.001; **: p<0.01; *: p<0.05; ns: non-significant.

FIGURE 4. Pearson's correlation between the evaluated vegetation indexes (VI) and leaf stomatal conductance (gs) for the cultivar BRS-8980. Teresina, PI, Brazil, 2019.

Soybean Leaf water potential (Ψf) was correlated with the spectral indexes evaluated by Wijewardana et al. (2019b). The indexes NDVI (r = 0.905), RNDVI (r = 0.905), NWI (r = 0.866), NWI4 (r = 0.843), and NWI5 (r = 0.742) increased linearly with increasing leaf Ψf values. In our study, this parameter showed a positive linear correlation with gs in soybean leaves (y = 0.94 + 0.60x, R2 = 0.6). NDVI had a higher correlation (r = 0.905) with leaf water potential than did the other VIs. Overall, NDVI is the index that best indicates soil cover by plant canopy (Zhao et al. 2007). Soil water stress reduces chlorophyll and other photosynthetic pigments, thus reducing the biomass and height of soybean plants, hence resulting in low NDVI values (Crusiol et al., 2017).

We observed that trend since NDVI and gs correlation reached only r = 0.576 (p <0.01). However, the indexes EVI, SAVI, RDVI, OSAVI, and NDRE, which use spectral bands in the NIR region, stood out in detecting soybean water status. This is because they allowed gs estimates with R^2 ranging from 0.462 (NIR) at 0.4506 (RDVI) and SSE from 108.1 (NIR) at 109.2 mmol H_2O m^{-2} s^{-1} (RDVI) (Figure 5). Wijewardana et al. (2019b) obtained a positive linear correlation between Ψf and NDVI, using the ratio y = 0.9495+0.08636x (y: NDVI ex: Ψf, in MPa) and R^2 = 0.82; therefore, NDVI can be used as a promising VI to detect soybean water status. Crusiol et al. (2017) also concluded that NDVI can be used as a soybean water status index, mainly at the reproductive stage, with potential for phenotyping and as a water deficit tolerance indicator.

Vegetation indexes and leaf nitrogen accumulation

Leaf N accumulations (NF) in the cultivar BONUS were significantly affected (p <0.05) by the WRs and N supplementation (NS) levels (Table 4). For the cultivar BRS-8980, the indexes CVI, EXGR, GLI, MEXG, MNGRD, NG, NGRD, and TGI responded to the N supplementation (NS) levels applied to the soil (p<0.001), while for the cultivar BONUS the indexes EXGR, GLI, MNGRD, NG, and NGRD stood out (p<0.01) (Table 4). These Vis, therefore, have the potential for N detection in soybeans; however, the promising VIs will be those with the best correlations with the NF measurements performed in the field.

Full irrigation promoted higher leaf N accumulations (6.4 g N m^{-2}) than did deficit irrigation (4.3 g N m^{-2}) (Figure 6). Nitrogen supplementation showed higher leaf N accumulation (5.5 g m^{-2}) compared to the absence of N application (5.2 g N m^{-2}) (Figure 6). The lowest leaf N accumulation (4.3 g N m^{-2}) was observed under deficit irrigation conditions (Figure 6). According to Chavarria et al. (2015), biological nitrogen fixation by soybeans may be compromised by soil water restriction, decreasing photosynthetic rates and hence final grain yields (Basal & Szabó, 2020).
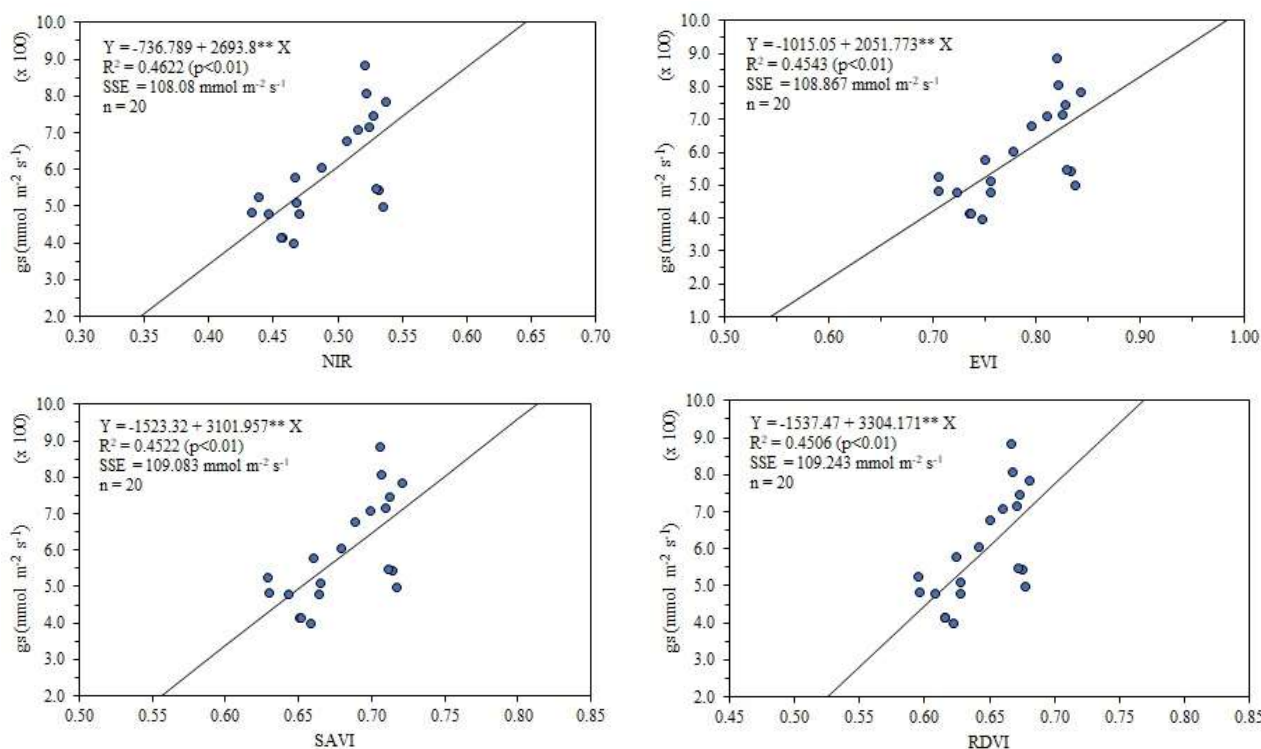
FIGURE 5. Regression between promising vegetation indexes and leaf stomatal conductance for the soybean cultivar BRS-8980. Teresina, PI, Brazil, 2019. Significance levels by t-test: ***: p<0.001; **: p<0.01; *: p<0.05; ns: non-significant.
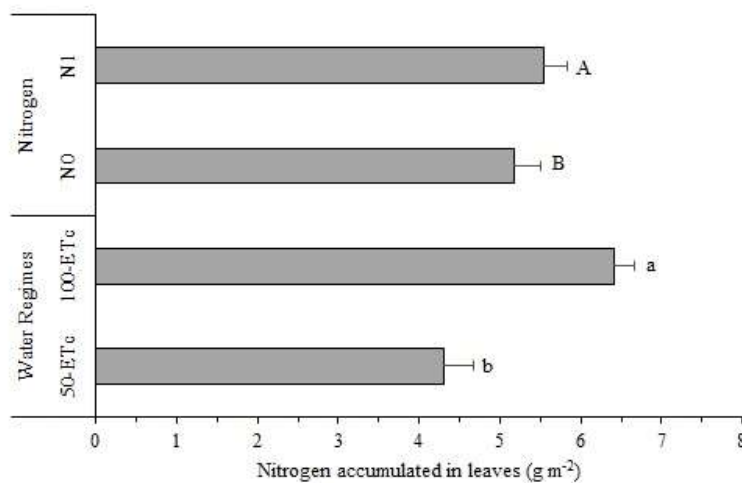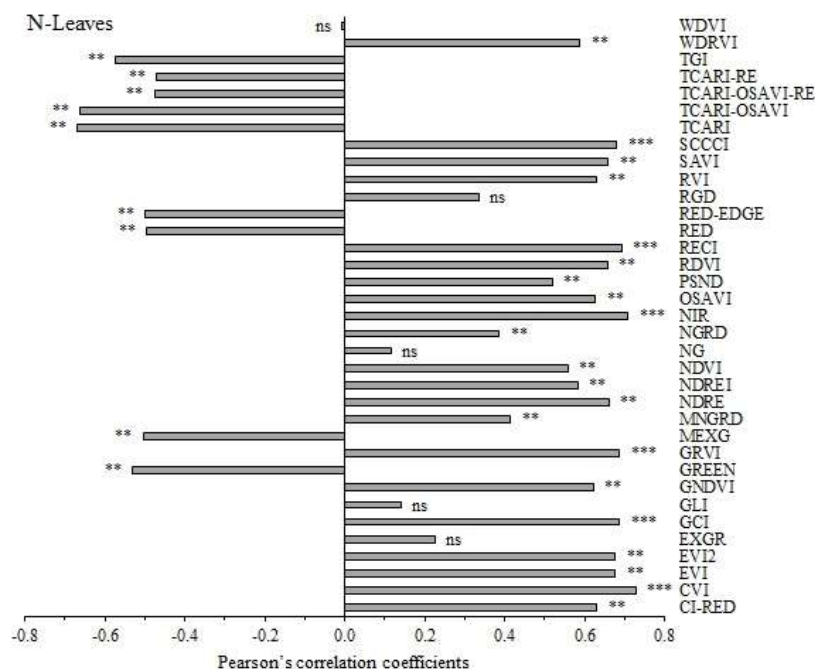

FIGURE 6. Leaf nitrogen accumulations in the soybean cultivar BONUS in response to the water regimes (WR) and nitrogen supplementation (NS) applied to the soil. Teresina, PI, Brazil, 2019. Means followed by the same letter do not differ from each other by the F-test (p<0.05). Lowercase (WR) and uppercase (NS) letters.

In a study performed in Piracicaba city - SP (Brazil) with the soybean cultivar RK7518 IPRO (indeterminate growth habit, average growth cycle, and maturation group 7.5), Zambon (2020) observed that leaf N accumulations reached maximum levels at the first phenological stages (64.2 g N kg^{-1}) and then had gradual reduction until the R6 stage (23.1 g N kg^{-1}). These authors observed a leaf N concentration of 27.3 g N kg^{-1} dry leaf biomass at the R5.2 stage (85 days after soybean emergence); as dry leaf biomass was 444.1 g m^{-2}, leaf N accumulation was 12.12 g N m^{-2}. This N accumulation was higher than that observed in our study under full irrigation (6.4 g N m^{-2}). This may be due to leaf dry biomass differences between both studies, as the cultivars had different cycles, maturation groups, and plant population stands.

Leaf N accumulation (NF) had significant correlations with several VIs evaluated in our study. Considering as promising the VIs with r≥0.6 (Yue et al., 2020), the six best ones for detecting leaf N accumulations were: CVI (r = 0.7266; p <0.001), NIR (r = 0.7065; p <0.001), RECI (r = 0.6912; p <0.001), GCI (r = 0.6869; p <0.001), GRVI (r = 0.6869, p <0.001), and SCCCI (r = 0.6795; p <0.001) (Figure 7). Moreover, for plant N contents, the same indexes stood out: CVI (r = 0.7601; p <0.001), GIT (r = -0.6923; p <0.001), SCCCI (r = 0.6803; p <0.001), RECI (r = 0.6749; p <0.001), GCI (r = 0.6733; p <0.001), and GRVI (r = 0.6733; p <0.001) (Figure 7).

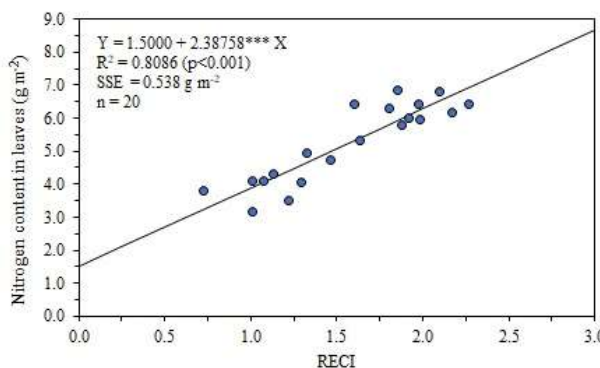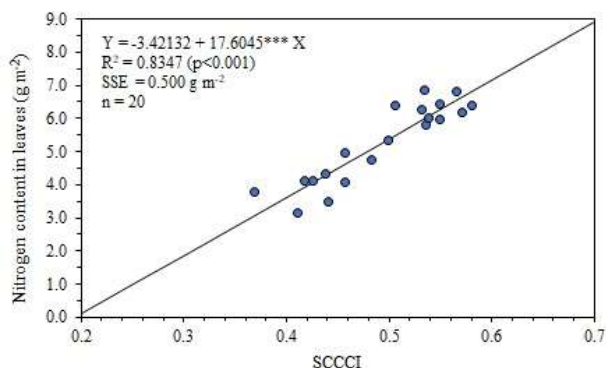Significance levels by the t-test: ***: p <0.001; **: p <0.01; *: p <0.05; ns: non-significant.
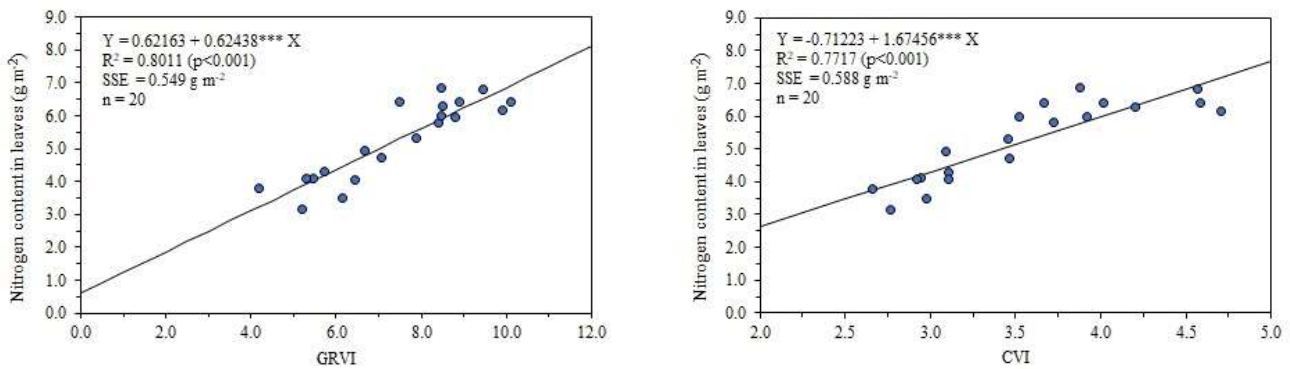
FIGURE 7. Pearson's correlation between vegetation indexes and leaf nitrogen accumulations for the soybean cultivar BONUS. Teresina, PI, Brazil, 2019.

Yue et al. (2020) evaluated soybean leaf chlorophyll contents using VIs from multispectral images and found that the best ones in terms of Pearson's correlation (r) were: TCARI/OSAVI-RE (r = 0.95; p <0.01), PSND (r = 0.88; p <0.01), and NDRE2 (r = 0.85; p <0.01). These authors concluded that soybean leaf chlorophyll contents are directly related to leaf N contents and emphasized that VI performance in detecting chlorophyll contents depends on soybean leaf area indexes. Therefore, the ratio between VI and chlorophyll content must be defined for different soybean phenological stages.

In our study, the indexes SCCCI, RECI, GRVI, CVI, TCARI-OSAVI, and TCARI promoted the best leaf N content estimates, with R^2 ranging from 0.8347 (p <0.001) to 0.7475 (p <0.001) and SSE from 0.500 g m^{-2} to 0.618 g m^{-2} (Figure 8). Such a superior performance of SCCCI in predicting leaf N contents has already been reported for other crops. For instance, among the numerous VIs evaluated by Raper & Varco (2015), SCCCI had the best correlation with leaf N contents in cotton (r = 0.787). As in our study, these authors found an increasing linear regression between SCCCI and leaf N contents ($R^2 = 0.62$). For wheat plants, Cammarano et al. (2011) also concluded that SCCCI has potential for leaf N content estimations (y = 0.94x + 0.15; R2 = 0.97; RMSE = 0.2 g N m^{-2}) and suggested future studies to validate its applicability under different production environments, sowing dates, and soil water conditions.

Significance levels by the t-test: ***: $p < 0.001$; **: $p < 0.01$; *: $p < 0.05$; ns: non-significant.

FIGURE 8. Linear regression between promising vegetation indexes and leaf nitrogen contents for the soybean cultivar BONUS. Teresina, PI, Brazil, 2019.

In a study with corn, Ciganda et al. (2009) found that RECI was a promising index to estimate leaf chlorophyll contents and reported a linear regression, with $R^2 = 0.9429$ and SSE = 50.9 mg N m^{-2} (y = 37.904+1353.7x). These authors highlighted a high linear correlation between model-estimated and field-observed chlorophyll contents ($R^2 = 0.9761$; RMSE = 37.5 mg N m^{-2}); thus, RECI has great potential for estimating leaf chlorophyll contents in corn plants.

CONCLUSIONS

The near-infrared spectral band and the vegetation indexes EVI, SAVI, and RDVI are promising for detecting soybean water status, while the indexes SCCCI, RECI, GRVI, and CVI are promising for estimating soybean nutritional status in terms of nitrogen contents.

REFERENCES

Allen RG, Pereira LS, Raes D, Smith M (1998) Crop evapotranspiration: Guidelines for computing crop water requirements. Rome, FAO. 300p. Drainage and Irrigation Paper, 56

Barbedo JGA (2019) A Review on the use of unmanned aerial vehicles and imaging sensors for monitoring and assessing plant stresses. Drones 3:1-27. DOI: https://doi: 10.3390/drones3020040

Baluja J, Diago MP, Balda P, Zorer R, Meggio F, Morales F, Tardaguila J (2012) Assessment of vineyard water status variability by thermal and multispectral imagery using an unmanned aerial vehicle (UAV). Irrigation Science 30:511-522. DOI: https://doi.org/10.1007/s00271-012-0382-9

Brar GS, Kar S, Singh NT (1990) Photosynthetic response of wheat to soil water deficits in the tropics. Journal of Agronomy and Crop Science 164:343–348. DOI: https://doi.org/10.1111/j.1439-037X.1990.tb01174.x

Basal O, Szabó A (2020) Ameliorating drought stress effects on soybean physiology and yield by hydrogen peroxide. Agriculturae Conspectus Scientificus 85(3):211-218. DOI: https://www.researchgate.net/publication/344235630

Bendig J, Yu K, Aasen H, Bolten A, Bennertz S, Broscheit J, Gnyp ML, Bareth G (2015) Combining UAV-based plant height from crop surface models, visible, and near-infrared vegetation indices for biomass monitoring in barley. International Journal of Applied Earth Observations 39:79-87. DOI: https://doi.org/10.1016/j.jag.2015.02.012

Bian J, Zhang Z, Chen J, Chen H, Cui C, Li X, Chen S, Fu Q (2019) Simplified evaluation of cotton water stress using high resolution unmanned aerial vehicle thermal imagery. Remote Sensing 11:267-274. DOI: https://doi.org/10.3390/rs11030267

Blackburn, GA (1998) Quantifying chlorophylls and carotenoids at leaf and canopy scales: An evaluation of some hyperspectral approaches. Remote Sensing of Environment 66:273-285. DOI: https://doi.org/10.1016/S0034-4257(98)00059-5

Burgos-Artizzu XP, Ribeiro A, Guijarro M, Pajares G (2011) Real-time image processing for crop/weed discrimination in maize fields. Computers and Electronics in Agriculture 75:337–346. DOI: https://doi.org/10.1016/j.compag.2010.12.011

Cammarano D, Fitzgerald G, Basso B, O'Leary G, Chen D, Grace P, Fiorentino C (2011) Use of the canopy chlorophyll content index (CCCI) for remote estimation of wheat nitrogen content in rainfed environments. Agronomy Journal 103(6):1597-1603. DOI: https://doi.org/10.2134/agronj2011.0124

Carvalho JFC, Crusiol LGT, Perini LJ, Sibaldelli RNR, Ferreira LC, Guimarães FCM, Nepomuceno AL, Neumaier N, Farias JRB (2015) Phenotyping soybeans for drought responses using remote sensing techniques and non-destructive physiological analysis. Global Science and Technology 8:1-16. DOI: https://doi.org/10.14688/1984-3801/gst.v8n2p1-16

Chavarria G, Durigon MR, Klein VA, Kleber H (2015) Photosynthetic restriction of soybean plants under varying water availability. Ciência Rural 45(8):1387-1393. DOI: https://doi.org/10.1590/0103-8478cr20140705

Ciganda V, Gitelson A, Schepers J (2009) Non-destructive determination of maize leaf and canopy chlorophyll content. Journal of Plant Physiology 166(2):157-167. DOI: https://doi.org/10.1016/j.jplph.2008.03.004

Clevers JGPW (1989) The application of a weighted infrared-red vegetation index for estimating leaf area index by correcting for soil moisture. Remote Sensing of Environment 29:25-37. DOI: https://doi.org/10.1016/0034-4257(89)90076-X

Colorado JD, Cera-Bornacelli N, Caldas JS, Petro E, Rebolledo MC, Cuellar D, Calderon F, Mondragon IF, Jaramillo-Botero A (2020) Estimation of nitrogen in rice crops from UAV-captured images. Remote Sensing 12(20):3396. DOI: https://doi.org/10.3390/rs12203396

Crusiol LGT, Carvalho JFC, Sibaldelli RNR, Neiverth W, Rio A, Ferreira LC, Procopio SO, Mertz-Henning LM, Nepomuceno AL, Neumaier N, Farias JRB (2017) NDVI variation according to the time of measurement, sampling size, positioning of sensor and water regime in different soybean cultivars. Precision Agriculture 18:470-490. DOI: https://doi.org/10.1007/s11119-016-9465-6

Crusiol LGT, Nanni MR, Furlanetto RH, Sibaldelli RNR, Cezar E, Mertz-Henning LM, Nepomuceno AL, Neumaier N, Farias JRB (2020) UAV-based thermal imaging in the assessment of water status of soybean plants. International Journal of Remote Sensing 41:3243-3265. DOI: https://doi.org/10.1080/01431161.2019.1673914

Daughtry CST, Walthall CL, Kim MS, Colstoun EB, McMurtrey JE (2000) Estimating corn leaf chlorophyll concentration from leaf and canopy reflectance. Remote Sensing of Environment 74:229-239. DOI: https://doi.org/10.1016/S0034-4257(00)00113-9

Elsayed S, Richneck P, Schmidhalter U (2015) Comparing the performance of active and passive reflectance sensors to assess the normalized relative canopy temperature and grain yield of drought-stressed barley cultivars. Field Crops Research 177:148-160. DOI: https://doi.org/10.1016/j.fcr.2015.03.010

Fehr WR, Caviness CE (1977) Stages of soybean development. Ames, Iowa State University, 12 p.

Ferreira EB, Cavalcanti PP, Nogueira DE (2018) ExpDes.pt: Experimental Design package (Portuguese). R package version 1.2.0. DOI: https://doi.org/10.4236/am.2014.519280

Franchini JC, Balbinot Junior AA, Jorge LAC, Debiasi H, Dias WP, Godoy AV, Oliveira Junior A, Correa FB, Oliveira MCN (2018) Uso de imagens aéreas obtidas com drones em sistemas de produção de soja. Londrina, Embrapa Soja, 2018. 39 p. Documentos / Embrapa Soja, 48. DOI: https://www.infoteca.cnptia.embrapa.br/infoteca/bitstream/doc/1103613/1/ Doc408OLalta.pdf

Gago J, Douthe C, Coopman RE, Gallego PP, Ribas-Carbo M, Flexas J, Escalona J, Medrano H (2015) UAVs challenge to assess water stress for sustainable agriculture. Agricultural Water Management 153:9–19. DOI: https://doi.org/10.1016/j.agwat.2015.01.020

Gitelson AA (2004) Wide dynamic range vegetation index for remote quantification of biophysical characteristics of vegetation. Journal of Plant Physiology 161:165-173. DOI: https://doi.org/10.1078/0176-1617-01176

Gitelson AA, Vina A, Ciganda V, Rundquist DC, Arkebauer TJ (2005) Remote estimation of canopy chlorophyll content in crops. Geophysical Research Letters 32:1-4. DOI: https://doi.org/10.1029/2005GL022688

Gorthi A, Volenec JJ, Welp LR (2019) Stomatal response in soybean during drought improves leaf-scale and field-scale water use efficiencies. Agricultural and Forest Meteorology 107629:276-277. DOI: https://doi.org/10.1016/j.agrformet.2019.107629

Haboudane D, Miller JR, Tremblay N, Zarco-Tejada PJ, Dextraze L (2002) Integrated narrow-band vegetation indices for prediction of crop chlorophyll content for application to precision agriculture. Remote Sensing of Environment 81:416-426. DOI: https://doi.org/10.1016/S0034-4257(02)00018-4

Hamuda E, Glavin M, Jones E (2016) A survey of image processing techniques for plant extraction and segmentation in the field. Computers and Electronics in Agriculture 125:184-199. DOI: https://doi.org/10.1016/j.compag.2016.04.024

Hassan MA, Mengjiao Y, Awais R, Xiuliang J, Xianchun X, Yonggui X, Zhonghu H (2018) Time-Series Multispectral Indices from Unmanned Aerial Vehicle Imagery Reveal Senescence Rate in Bread Wheat. Remote Sensing 10:809-818. DOI: https://doi.org/10.3390/rs10060809

Hoffmann H, Jensen R, Thomsen A, Nieto H, Rasmussen J, Friborg T (2016) Crop water stress maps for an entire growing season from visible and thermal UAV imagery. Biogeosciences 13:6545–6563. DOI: https://doi.org/10.5194/bg-13-6545-2016

Hoyos-Villegas V, Fritschi, FB (2013) Relationships among vegetation indices derived from aerial photographs and soybean growth and yield. Crop Science 53:2631-2642. DOI: https://doi.org/10.2135/cropsci2013.02.0126

Huete A, Didan K, Miura T, Rodriguez EP, Gao X, Ferreira LG (2002) Overview of the radiometric and biophysical performance of the MODIS vegetation indices. Remote Sensing of Environment 83:195–213. DOI: https://doi.org/10.1016/S0034-4257(02)00096-2

Hungria M, Campo RJ, Mendes IC (2001) Fixação biológica do nitrogênio na soja. Londrina, Embrapa Soja. 48p. Circular Técnica, 35. DOI: https://ainfo.cnptia.embrapa.br/digital/bitstream/CNPSO/18515/1/circTec35.pdf

Hunt ER, Daughtry CST (2018) What good are unmanned aircraft systems for agricultural remote sensing and precision agriculture? International Journal of Remote Sensing 39:5345–5376. DOI: https://doi.org/10.1080/01431161.2017.1410300

Hunt ERJ, Daughtry, CST, Eitel JUH, Long DS (2011) Remote sensing leaf chlorophyll content using a visible band index. Agronomy Journal 103:1090-1099. DOI: https://doi.org/10.2134/agronj2010.0395

Hunt ER, Doraiswamy PC, McMurtrey JE, Daughtry CST, Perry EM, Akhmedov B (2013) A visible band index for remote sensing leaf chlorophyll content at the canopy scale. International Journal of Applied Earth Observations 21:103–112. DOI: https://doi.org/10.1016/j.jag.2012.07.020

INMET - Instituto Nacional de Meteorologia. Dados históricos: 2019. Available at: https://portal.inmet.gov.br/dadoshistoricos. Accessed on Apr. 30, 2020.

Jiang Z, Huete A, Miura T, Didan K (2008) Development of a two-band enhanced vegetation index without a blue band. Remote Sensing of Environment 112:3833-3845. DOI: https://doi.org/10.1016/j.rse.2008.06.006

Karaca C, Tekelİoglu B, Buyuktas D, Bastug R (2018) Relations between crop water stress index and stomatal conductance of soybean depending on cultivars. Fresenius Environmental Bulletin 27(6):4212-4219.

Kaschuk G, Hungria M, Leffelaar PA, Giller KE, Kuyper TW (2010) Differences in photosynthetic behavior and leaf senescence of soybean (Glycine max [L.] Merrill) dependent on N2 fixation or nitrate supply. Plant Biology 12:60-69. DOI: https://doi.org/10.1111/j.1438-8677.2009.00211.x

Machado Júnior CS, Silva CR, Sanches MC, Hamawaki OT, Sousa LB (2017) Physiologic parameters of soybean of determinate and indeterminate growth habit subjected to levels of soil moisture. Pesquisa Agropecuária Brasileira 52(6):419-425. DOI: https://doi.org/10.1590/S0100-204X2017000600005

Machado ML, Simão MLR, Simão FR, Alexandrino, RCS (2020) Stress conditions in soybean areas based on measurements of soil-plant-atmosphere system and UAV images. Pesquisa Agropecuária Tropical 50:e61785. DOI: https://doi.org/10.1590/1983-40632020v5061785.

Maimaitijiang M, Ghulam A, Sidike P, Hartling S, Maimaitiyiming M, Peterson K, Shavers E, Fishman J, Peterson J, Kadam S, Burken J, Fritschi F (2017) Unmanned Aerial System (UAS)-based phenotyping of soybean using multi-sensor data fusion and extreme learning machine. ISPRS Journal of Photogrammetry and Remote Sensing 134:43-58. DOI: https://doi.org/10.1016/j.isprsjprs.2017.10.011

Manalavan LP, Guttikonda SK, Tran LP, Nguyen HT (2009) Physiological and molecular approaches to improve drought resistance in soybean. Plant and Cell Physiology 50:1260–1276. DOI: https://doi.org/10.1093/pcp/pcp082

Medeiros MR, Cavalcanti EP, Duarte JFM (2020) Classificação climática de Köppen para o Estado do Piauí-Brasil, Revista Equador (UFPI) 9:82-99. DOI: http://www.ojs.ufpi.br/index.php/equador

Melo FB, Andrade Junior AS, Pessoa BLO (2014) Levantamento, zoneamento e mapeamento pedológico detalhado da área experimental da Embrapa Meio-Norte em Teresina, PI. Teresina: Embrapa Meio-Norte, 34p. Documentos 231. DOI: https://ainfo.cnptia.embrapa.br/digital/bitstream/item/120989/1/Doc-231.pdf

Meyer GE, Camargo Neto J (2008) Verification of color vegetation indices for automated crop imaging applications. Computers and Electronics in Agriculture 63:282-293. DOI: https://doi.org/doi:10.1016/j.compag.2008.03.009

QGIS Development Team. 2021. QGIS user guide, Release 3.16. Available at: https://docs.qgis.org/3.16/en/docs/index.html. Accessed on Mar. 20, 2021.

Raper TB, Varco JJ (2015) Canopy-scale wavelength and vegetative index sensitivities to cotton growth parameters and nitrogen status. Precision Agriculture 16:62-76. DOI: https://doi.org/10.1007/s11119-014-9383-4

Reddy AR, Chaitanya KV, Vivekanandan M (2004) A review: drought-induced responses of photosynthesis and antioxidant metabolism in higher plants. Journal of Plant Physiology 161:1189–1202. DOI: https://doi.org/10.1016/j.jplph.2004.01.013

Roujean JL, Breon FM (1995) Estimating PAR absorbed by vegetation from bidirectional reflectance measurements. Remote Sensing of Environment 51:375–384. DOI: https://doi.org/10.1016/0034-4257(94)00114-3

Rondeaux G, Steven M, Baret F (1996) Optimization of soil adjusted vegetation indices. Remote Sensing of Environment 55:95-107. DOI: https://doi.org/10.1016/0034-4257(95)00186-7

Sagan V, Maimaitijiang M, Sidike P, Eblimit K, Kyle P, Sean H, Flavio E, Kapil K, Newcomb M, Pauli W, Ward R, Fritschi Felix, Shakoor N, Mockler T (2019) UAV-based high-resolution thermal imaging for vegetation monitoring, and plant phenotyping using ICI 8640 P, FLIR Vue Pro R 640, and thermoMap cameras. Remote Sensing 11(3):330-359. DOI: https://doi.org/10.3390/rs11030330

Sanjerehei, MM (2014) Assessment of spectral vegetation indices for estimating vegetation cover in arid and semiarid shrublands. Range Management Agroforest 35(1):91–100. DOI: https://www.cabdirect.org/cabdirect/abstract/20143381736

Silva SP (2021) Crescimento e produtividade da soja em resposta a adubação nitrogenada com e sem deficiência hídrica. Dissertação, Teresina. Universidade Federal do Piauí

Silva JA, Santos PAB, Carvalho LG, Moura EG, Andrade FR (2020) Gas exchanges and growth of soybean cultivars submitted to water deficiency. Pesquisa Agropecuária Tropical 50:e58854. DOI: https://doi.org/10.1590/1983-0632020v5058854

Sripada RP, Heiniger RW, White J, Meijer AD (2006) Aerial color infrared photography for determining early in-season nitrogen requirements in corn. Agronomy Journal 98:968-977. DOI: https://doi.org/10.2134/agronj2005.0200

Teixeira PC, Donagemma GK, Fontana A, Teixeira WG (2017) Manual de métodos de análise de solo. Brasília, DF, Embrapa, p368-376.

Tetila EC, Machado BB, Belete NA, Guimaraes DA, Pistori H (2017) Identification of soybean foliar diseases using unmanned aerial vehicle images. IEEE Geoscience and Remote Sensing Letters 14(12):2190-2194. DOI: https://doi.org/10.1109/LGRS.2017.2743715

Thomas AL (2018) Soja: tipos de crescimento da planta. Porto Alegre, Universidade Federal do Rio Grande do Sul-UFRGS, 2018. 59p.

Tucker CJ (1979) Red and photographic infrared linear combinations for monitoring vegetation. Remote Sensing of Environment 8:127-150. DOI: https://doi.org/10.1016/0034-4257(79)90013-0

Vibhute A, Bodhe SK (2012) Applications of image processing in agriculture: a survey. International Journal of Computer Applications 52:34-40. DOI: https://doi.org/10.5120/8176-1495

Vincini M, Frazzi E, D'Alessio P (2008) A broad-band leaf chlorophyll vegetation index at the canopy scale. Precision Agriculture 9:303–319. DOI: https://doi.org/10.1007/s11119-008-9075-z

Wang W, Vinocur B, Altman A (2003) Plant responses to drought, salinity, and extreme temperatures towards genetic engineering for stress tolerance. Planta 218:1–14. DOI: https://doi.org/ 10.1007/s00425-003-1105-5

Wang S, Azzari G, Lobell DB (2019) Crop type mapping without field-level labels: Random forest transfer and unsupervised clustering techniques. Remote Sensing of Environment 222:303–317. DOI: https://doi.org/10.1016/j.rse.2018.12.026

Wijewardana C, Reddy KR, Alsajri FA, Irby T, Krutz J, Golden B (2018) Quantifying soil moisture deficit effects on soybean yield and yield component distribution patterns. Irrigation Science 36:241–255. DOI: https://doi.org/ 10.1007/s00271-018-0580-1

Wijewardana C, Reddy KR, Bellaloui N (2019a) Soybean seed physiology, quality, and chemical composition under soil moisture stress. Food Chemistry 278:92–100. DOI: https://doi.org/ 10.1016/j.foodchem.2018.11.035

Wijewardana C, Alsajri FA, Irby JT, Krutz LJ, Golden B, Henry WB, Gao W, Reddy KR (2019b) Physiological assessment of water deficit in soybean using midday leaf water potential and spectral features. Journal of Plant Interactions 14:533-543. DOI: https://doi.org/10.1080/17429145.2019.1662499

Woebbecke DM, Meyer GE, Bargen KV, Mortensen DA (1995) Color indices for weed identification under various soil, residue, and lighting conditions. Trans. ASAE 38(1):259-269. DOI: https://doi.org/10.13031/2013.27838

Yu N, Li L, Schmitz N, Tian LF, Greenberg JA, Diers BW (2016) Development of methods to improve soybean yield estimation and predict plant maturity with an unmanned aerial vehicle-based platform. Remote Sensing of Environment 187:91-101. DOI: https://doi.org/10.1016/j.rse.2016.10.005

Yue J, Feng H, Tian Q, Zhou C (2020) A robust spectral angle index for remotely assessing soybean canopy chlorophyll content in different growing stages. Plant Methods 16:104-122. DOI: https://doi.org/10.1186/s13007-020-00643-z

Zambon LM (2020) Caracterização do crescimento e acúmulo de nitrogênio em uma cultura de soja de elevada produtividade. Dissertação Mestrado, Universidade de São Paulo, Escola Superior de Agricultura "Luiz de Queiroz.

Zaiontz C (2020) Real Statistics Using Excel. Available at: www.real-statistics.com. Accessed on Mar. 05, 2020.

Zhao D, Reddy KR, Kakani VG, Read JJ, Koti S (2007) Canopy reflectance in cotton for growth assessment and lint yield prediction. European Journal of Agronomy 26:335–344. DOI: https://doi.org/10.1016/j.eja.2006.12.001

Zhong L, Hu L, Zhou H (2019) Deep learning-based multi-temporal crop classification. Remote Sensing of Environment 221:430–443. DOI: https://doi.org/ 10.1016/j.rse.2018.11.032